JOURNAL OF SYNCHROTRON RADIATION

**Volume 22 (2015)**

**Supporting information for article:**

# Direct nano-scale patterning of Ag films using hard X-ray induced oxidation

**Jae Myung Kim, Su Yong Lee, Hyon Chol Kang and Do Young Noh**

# Supplementary Information : Direct nano-scale patterning of Ag films using hard x-ray induced oxidation

Jae Myung Kim, Su Yong Lee, Hyon Chol Kang, and Do Young Noh

## I. BEHAVIOR OF SILVER NANOPARTICLES DURING X-RAY EXPOSURE UNDER OXYGEN-FREE ENVIRONMENT

There was no significant change in AgNPs exposed to hard x-rays under oxygen free environments. AgNPs exposed to hard x-rays under vacuum, nitrogen, hydrogen mixed argon, or carbon dioxide ambient showed little change as compared to the as-grown samples. (Figure S1) This result confirmed that oxygen played major role in the observed behavior of AgNPs under hard x-ray irradiation.

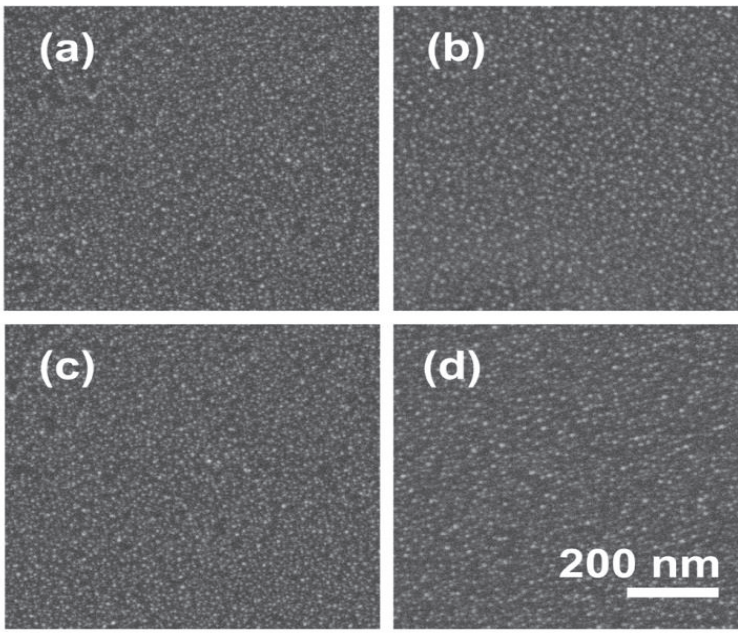


Fig. S 1. SEM images of x-ray irradiated AgNPs under vacuum ($3 \times 10^{-4}$Torr)(a), 760 Torr of $N_2$ (b) $CO_2$ (c) and hydrogen(2 %) mixed Argon(98 %) ambient respectively. The x-ray exposure was 28 min. No noticeable change was observed.

## II. SILVER NANOPARTICLES EXPOSED TO HARD X-RAYS IN AIR WITH WATER VAPOR

Shown in Figure S2(a) are SEM images of the AgNPs exposed to hard x-ray beam in air of 18% and 78% relative humidity. During The AgNPs exposed by hard x-rays under air ambient at one atmospheric pressure diffused and agglomerated to form clusters of AgNPs. As shown in the SEM images as well as the particle density estimated from them, the speed of the process was higher in air with water molecules than in oxygen. With increasing the humidity, the agglomeration and diffusion became faster. This result implies that it is easier to break water molecules than oxygen molecules with hard x-ray photons.

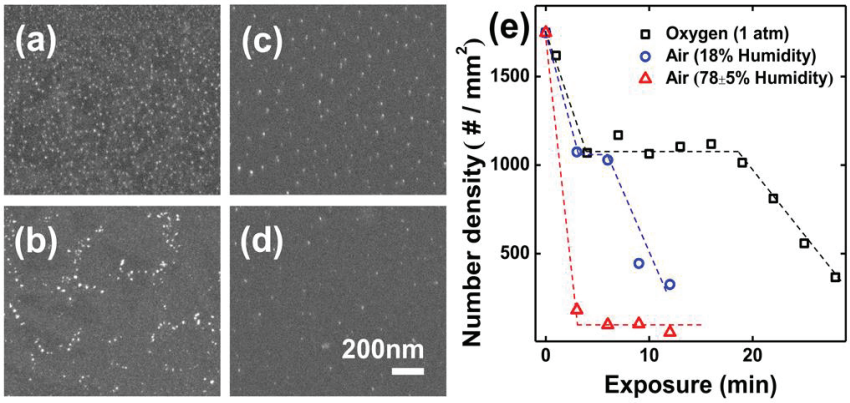


Fig. S 2. (a,b) Morphology of AgNPs exposed to x-rays in air with 18% relative humidity for 6 and 12 min, respectively. (c,d) Morphology of x-ray AgNPs exposed to x-rays in air with 78% relative humidity for 6 and 12 min. (e) Change of the particle number density as a function of time. At 78±5% relative humidity, the number density change of AgNPs was faster than other conditions.

## III. X-RAY DIFFRACTION PEAKS OF AG OXIDE

Since the diffraction peak of the disordered silver oxide nano-particles in the specimens used in this paper was too weak to detect, the oxidation of Ag was not directly confirmed, although we observed the disappearance of the Ag(111) peak. To confirm the formation of Ag oxides, we fabricated a thicker Ag film and exposed to x-rays in the similar configuration as described in the manuscript. Figure S 3 shows the growth AgO and $Ag_2O$ Bragg peak with increasing the exposure to hard x-ray beam.

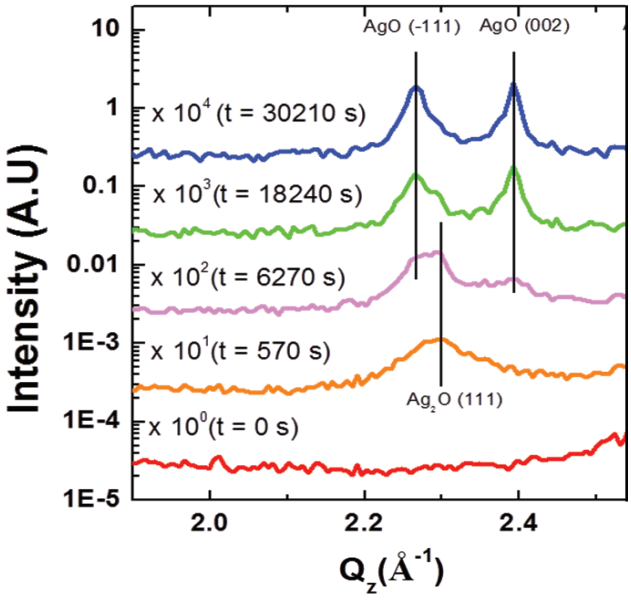


Fig. S 3. Formation of the AgO ($\bar{1}11$), AgO(002), and $Ag_2O$(111) Bragg peaks as a silver film grown on sapphire substrate was exposed to hard x-ray beam

## IV. ESTIMATION OF THE HARD X-RAY FLUX

In the hard x-ray induced nano-scale pattering of AgNPs, the flux of hard x-ray is one of the key controlling variables. We used an undulator beamline at PLS-II (Pohang Light Source II, Korea) synchrotron for this experiment. The x-ray energy of 7.5 keV was selected by a double crystal Si monochromator with energy band width of $\Delta E/E \sim 10^{-4}$. We focused x-ray beam using a Fresnel zone plate (FZP) with 364 zones whose outermost zone width was 400 nm. A pair of guard slits was installed upstream of the FZP to define the incident x-ray beam to about 600 m both in vertical and horizontal directions matching the dimension of the FZP. The focal length of the FZP at this x-ray energy was 1.47 m. The measured beam size at the focus was 4.3 $\mu$m and 18.7 $\mu$m in the vertical and horizontal direction respectively. The anisotropic dimension of the focused beam was resulted from the anisotropy in the x-ray beam coherency and the source size.

The flux of unfocused x-ray beam was estimated using the photo current measured with an x-ray sensitive photodiode. The following parameters were used in the estimation.

- Photo-current : $5 \times 10^{-}5$ A (measured by photodiode)
- Quantum efficiency : electron-hole pairs/3.63 eV
- Photon energy : 7.5 keV

- Air scattering length: 45cm (Transmission : 0.534)
- Al filter to block photodiode: Transmission : 0.78
- Beam size defined by slit: 600 $\mu$m $\times$ 600 $\mu$m

$\rightarrow$ Photon flux of unfocused incident beam
$= 5 \times 10^{-6} \times (3.63/7500)/1.6 \times 10^{-19}/0.78/0.534/0.6/0.6$
$\sim 1 \times 10^{12} photons/sec/mm^2$

Considering that the focusing efficiency of the FZP used in this experiment was about 16%, we estimate that the photon flux at the focus was about $7 \times 10^{14} photons/sec/mm^2$ with the following values.

$\rightarrow$ Photon flux at focus
$=$ Flux of unfocused beam $\times$ beam size at FZP
$\times$ FZP efficiency / Focused beam size
$\sim 7 \times 10^{14} photons/sec/mm^2$